MBoC | ARTICLE

γ-tubulin complex controls the nucleation of tubulin-based structures in Apicomplexa

Romuald Haase, Annet Puthenpurackal, Bohumil Maco, Amandine Guérin*, and Dominique Soldati-Favre*

Department of Microbiology and Molecular Medicine, Faculty of Medicine, University of Geneva, CH-1221 Geneva 4, Switzerland

ABSTRACT **Apicomplexan parasites rely on tubulin structures throughout their cell and life cycles, particularly in the polymerization of spindle microtubules to separate the replicated nucleus into daughter cells. Additionally, tubulin structures, including conoid and subpellicular microtubules, provide the necessary rigidity and structure for dissemination and host cell invasion. However, it is unclear whether these tubulin structures are nucleated via a highly conserved γ-tubulin complex or through a specific process unique to apicomplexans. This study demonstrates that *Toxoplasma* γ-tubulin is responsible for nucleating spindle microtubules, akin to higher eukaryotes, facilitating nucleus division in newly formed parasites. Interestingly, γ-tubulin colocalizes with nascent conoid and subpellicular microtubules during division, potentially nucleating these structures as well. Loss of γ-tubulin results in significant morphological defects due to impaired nucleus scission and the loss of conoid and subpellicular microtubule nucleation, crucial for parasite shape and rigidity. Additionally, the nucleation process of tubulin structures involves a concerted action of γ-tubulin and Gamma Tubulin Complex proteins (GCPs), recapitulating the localization and phenotype of γ-tubulin. This study also introduces new molecular markers for cytoskeletal structures and applies iterative expansion microscopy to reveal microtubule-based architecture in *Cryptosporidium parvum* sporozoites, further demonstrating the conserved localization and probable function of γ-tubulin in *Cryptosporidium*.**

SIGNIFICANCE STATEMENT

- Apicomplexan parasites harbor distinctive tubulin-based structure crucial for parasite shape, motility and invasion. The mechanisms underlying their biogenesis remain enigmatic.
- The researchers combined ultrastructure-expansion microscopy (U-ExM) and genome editing in *Toxoplasma gondii* to investigate the localization and function of γ tubulin and Gamma Tubulin Complex proteins (GCPs). Gamma tubulin and GCPs regulate the nucleation of spindle microtubules, conoid tubulin fibers, and subpellicular microtubules.
- Additionally, in *Cryptosporidium parvum*, U-ExM provided insight into its tubulin cytoskeleton organization and nucleation. These findings underscore the conserved mechanism of microtubule nucleation in Apicomplexa that orchestrates the production of tubulin-based structures in a tightly controlled temporal and spatial manner.

Monitoring Editor
Isabelle Coppens
Johns Hopkins Malaria Research Institute

Received: Mar 6, 2024
Revised: Jun 26, 2024
Accepted: Jul 18, 2024

Cross-Species

This article was published online ahead of print in MBoC in Press (http://www.molbiolcell.org/cgi/doi/10.1091/mbc.E24-03-0100) on July 24, 2024.

Author contributions: D.S-F., R.H., and A.G. conceptualized the project and methodology. R.H., A.G., B.M., and A.P. performed the investigations. R.H., A.G., and A.P. did the formal analysis. R.H. and A.P. wrote the original draft. D.S-F., A.G., and A.P. reviewed and edited the manuscript. D.S-F. and A.G. did the funding acquisition and obtained resources. All authors contributed to this article and approved the submitted version.

Competing interests: The authors declare no competing interests.

*Address correspondence to: Amandine Guérin (amandine.guerin@unige.ch); Dominique Soldati-Favre (dominique.soldati-favre@unige.ch).

Abbreviations used: GCPs, Gamma Tubulin Complex proteins; IMC, inner membrane complex; ICMTs, intraconoidal microtubules; SPMTs, subpellicular microtubules; U-ExM, ultrastructure-expansion microscopy.

INTRODUCTION

The phylum of Apicomplexa encompasses thousands of species ranging from free-living to intracellular parasites, including pathogens responsible for human diseases such as *Cryptosporidium* (cryptosporidiosis), *Plasmodium* (malaria) and *Toxoplasma gondii* (toxoplasmosis). To invade host cells, these obligate intracellular parasites rely on gliding motility machinery powered by its actomyosin system and the secretion of specialized organelles termed rhoptries and micronemes (Opitz and Soldati, 2002; Green *et al*., 2017; Dubois and Soldati-Favre, 2019; Ben Chaabene *et al*., 2020; Guérin *et al*., 2021; Dos Santos Pacheco *et al*., 2022; Martinez *et al*., 2023).

T. gondii exhibits a remarkable ability to invade virtually all types of nucleated cells in warm-blooded animals. Upon invasion, the parasite resides within a parasitophorous vacuole (PV) and undergoes division through endodyogeny, a process where two daughter cells form within the mother cell (Gubbels *et al*., 2020). The centrosomes serve as a hub to nucleate the spindle microtubules during mitosis and orchestrate the assembly of daughter cell components, including the cortical cytoskeleton (Suvorova *et al*., 2015; Morlon-Guyot *et al*., 2017).

In contrast, *Cryptosporidium* parasite replicates by schizogony where three successive rounds of highly coordinated and synchronous nuclear divisions give rise to eight nuclei, followed by segmentation (English *et al*., 2022). Despite the importance of this process, the biogenesis of tubulin-based structures during *Cryptosporidium* replication remains poorly understood (Wang *et al*., 2021).

Gamma tubulin (γ-tubulin) is a highly conserved and essential protein in eukaryotes, required for microtubule nucleation (Oakley *et al*., 2015). A dimer of γ-tubulin assembles in the centrosome with additional Gamma Tubulin Complex proteins (GCPs) to form γ-TuSCs (γ-tubulin small complexes; Zheng *et al*., 1995). Following this association, γ-TuSCs and additional GCPs assemble into large γ-TuRCs (γ-tubulin ring complexes), providing the crucial structure needed for microtubule nucleation (Thawani and Petry, 2021; Aher *et al*., 2023). The conservation of γ-tubulin in eukaryotic organisms underscores its significance in cell division. Both *Toxoplasma* and *Cryptosporidium* possess essential tubulin-based structures of unclear origin, including centrioles, conoid fibers, subpellicular microtubules (SPMTs), and intraconoidal microtubules (ICMTs, in *T. gondii*; Dos Santos Pacheco *et al*., 2020, 2024, Tell i Puig and Soldati-Favre 2024).

In this study, we elucidate the dynamic localization of γ-tubulin during the cell cycle in *T. gondii*. Using U-ExM, we uncover the transient association of γ-tubulin with the nascent apical complex providing evidence of tubulin structure nucleation. Moreover, γ-tubulin depleted parasites die due to a failure of nuclei separation and cytoskeleton formation. In addition, the absence of γ-tubulin results in the formation of abnormally long microtubules emerging from collapsing centrosomes, which exhibit SPMT-like properties such as polyglutamylation and IMC budding. Our findings establish that the nucleation activity relies on the coordinated action of γ-tubulin and GCP proteins as evidenced by the localization and phenotype of GCP2 and 3 depleted parasites mirroring those of γ-tubulin-depleted ones. Significantly, we show that the dynamic localization of γ-tubulin and spindle microtubule formation follows a similar pattern in *Cryptosporidium parvum*, which divides in a different process compared to *T. gondii*, underlying the crucial function of γ-tubulin in apicomplexan. Furthermore, through iterative expansion microscopy (iUExM) coupled with new available molecular markers, we reveal the entire tubulin cytoskeleton of *C. parvum* sporozoites.

RESULTS

Toxoplasma gondii γ-tubulin transiently associates with the nascent apical complex

T. gondii tachyzoites divide by a process known as endodyogeny, characterized by the formation of two daughter cells within the mother cell. The initiation of endodyogeny involves the duplication of the centrioles, pivotal components of the centrosome (Figure 1). The duplicated centrioles connect to the centrosome, a conical structure linking the replicated nucleus to the centrosomes via the mitotic spindle (Figure 1). Concurrently, the nascent apical complex consisting of the conoid, ICMTs and SPMTs begins to emerge near the duplicated centrioles in a synchronous and circular manner (Padilla *et al*., 2024). As the division proceeds, daughter cell components, including the secretory organelles and the inner membrane complex (IMC) are synthesized and accumulate adjacent to the growing tubulin cytoskeleton. Finally, constriction occurs, leading to formed daughter cells, each that encapsulates their nucleus and organelles within the cell body (Figure 1).

To investigate the localization of γ-tubulin throughout the cell cycle, we employed an endogenous tagging approach by inserting a mini-auxin inducible degron sequence (mAiD) alongside a 3HA-epitope tag in the 3'UTR (Supplemental Figure 1A). Immunostaining of γ-tubulin displays a highly dynamic pattern throughout the cell cycle. In intracellular nondividing parasites, the γ-tubulin signal appears very weak and almost undetectable (Figure 2A). As parasites proceed to divide, first, a single punctum of γ-tubulin is detected. Subsequently, two close puncta can be observed with continuous staining between them, presumably reflecting centrosome duplication (Figure 2A). The two puncta gradually separate until the budding of the IMC eventually starts, at which point the γ-tubulin signal becomes faint and disperses throughout the cytosol (Figure 2A). Notably, in extracellular parasites, ~40% of tachyzoites retained punctate staining while the others showed a dispersed cytosolic staining pattern (Figure 2B; Supplemental Figure 2A). We compared the staining of γ-tubulin to another early daughter marker, Pcr4, in extracellular Pcr4-mAID-HA parasites, however, the absence of signal indicated no active daughter cell formation (Supplemental Figure 2B).

In *T. gondii*, the centrosome architecture consists of an outer core (distal) and an inner core (proximal) (Suvorova *et al*., 2015). The centrioles, along with the centrin1 protein, are part of the outer core. Dual labelling of γ-tubulin and centrin1 suggests that both proteins localize to the outer core of the centrosome as previously reported (Suvorova *et al*., 2015; Supplemental Figure 2C). To increase the resolution of the molecular organization of the centrosome, we applied ultrastructure expansion microscopy (U-ExM) applied to intracellular and extracellular parasites, (Figure 2B). In extracellular, a punctum of γ-tubulin was observed between the two centrioles while the centrin1 "fiber-like" structure was bridging the two centrioles (Figure 2B). The same organization was observed for intracellular parasites before centrosome duplication (Figure 2B). However, after centrosome duplication, centrin1 still bridged the two centrioles, while γ-tubulin localized on both sides of the nascent spindle microtubules as well as surrounding the centrioles (Figure 2B) Interestingly, despite the dense proteinaceous nature of the centrosome, γ-tubulin-mAiD-HA protein was found soluble in PBS as well as in RIPA and Cytoskeletal buffers (Supplemental Figure 2D).

Remarkably, as the endodyogeny continues, γ-tubulin associated with the nascent apical complex (conoid, ICMTs, and SPMTs) as well as close to the centriole and on both sides of the mitotic spindle as indicated by the acetylated tubulin staining (Figure 2C). Importantly, during the forming apical complex γ-tubulin staining

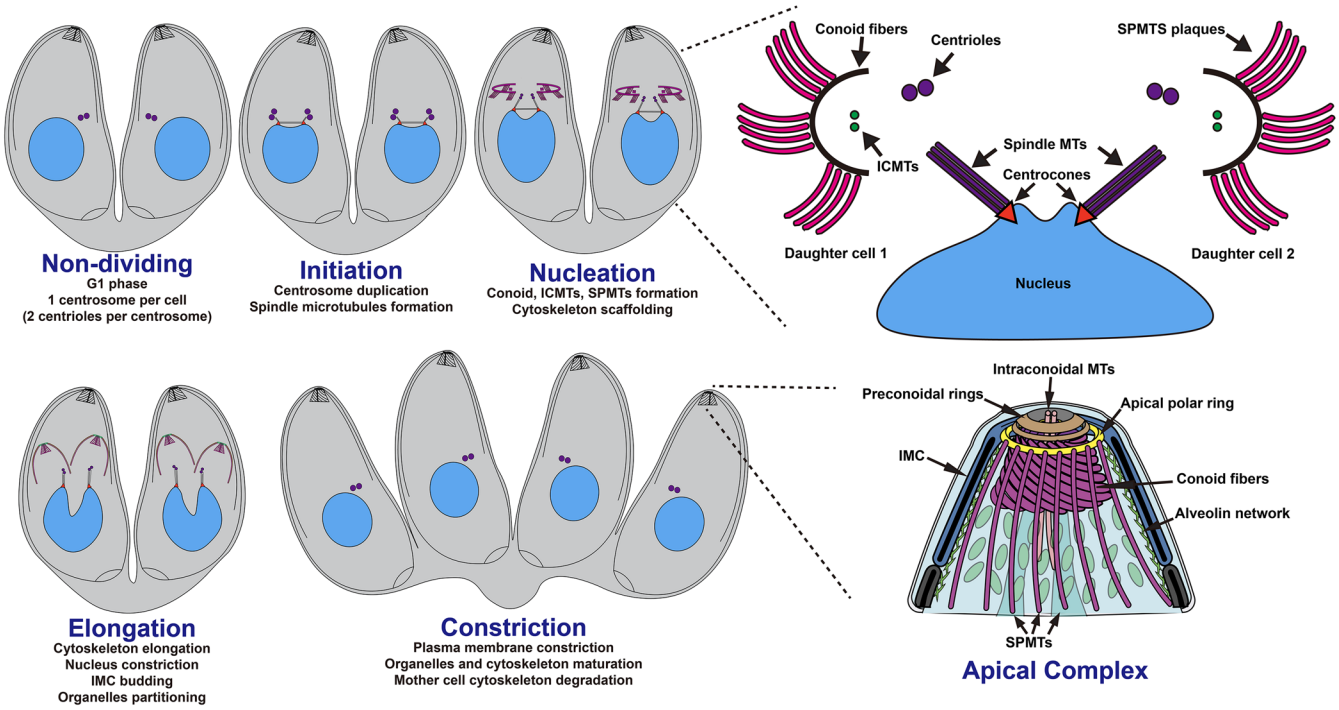

FIGURE 1: *Toxoplasma gondii* cytoskeletal organization during endodyogeny. Schematic representation of the endodyogeny process of *T. gondii*. Upper right corner: zoom on the nucleation with focus on the circular formation of the apical complex. Lower right corner: zoom on the fully developed apical complex.

was observed on the opposite side of the already formed part, highlighting its crucial role in the nucleation of these tubulin-based structures (Figure 2D).

Loss of *T. gondii* γ-tubulin leads to major morphological abnormalities due to defects in nucleus scission and cytoskeleton formation

To assess the γ-tubulin function in *T. gondii* life cycle, we employed the mAiD system for conditional downregulation at the protein level. Parasites depleted of γ-tubulin for 7 d failed to form plaque in the fibroblast monolayers, revealing the essential role of the gene for the parasite lytic cycle (Figure 3A). The γ-tubulin protein depletion exhibited fast regulation within 1 h (Figure 3B).

To dissect the role of γ-tubulin in the cell cycle, parasites were allowed to replicate for 12 to 14 h in the presence or absence of auxin. *T. gondii* parasites depleted for γ-tubulin display significant morphological defect, adopting a "bulbous" shape, defined by the IMC1 signal (Figure 3C). Although the production of new microtubules represented by the acetylated tubulin staining appears highly reduced, some signals could still be detected. Strikingly, parasites continue to produce new daughter cell material such as IMC and secretory organelles (micronemes and rhoptries), which became mislocalized and dispersed (Figure 3C). Additionally, γ-tubulin depletion results in the failure of apicoplast scission that appears fragmented, as well as the centrosome duplication with an odd number of centrin1 puncta (Figure 3C). Moreover, the enlarged replicated nucleus is unable to divide, likely due to the lack of spindle microtubule formation (Figure 3C).

To investigate the cause of the bulbous shape, intracellular γ-tubulin depleted parasites were examined by U-ExM. Short-time treated parasites showed no centriole duplication, while sparks of microtubules emerged from these unduplicated centrioles (white arrows; Figure 3D). With prolonged auxin treatment, these sparks of microtubules, still connected to the centrioles, elongated to abnormally long filaments, causing the parasite's tubulin cytoskeleton to lose its typical polarized shape (Figure 3D). Eventually, the classical cytoskeleton architecture of *T. gondii* becomes unrecognizable and extremely long microtubules are observed twirling around. Interestingly, while centriole duplication is blocked, the two original centrioles separate from each other, leading to a fragmented centrin1 staining that appears with multiple dots in these defective parasites. (Supplemental Figure 2E)

To gain further information, we employed electron microscopy to image the cellular abnormalities of the γ-tubulin depleted parasites. Layers of IMC budding were observed appearing in the cytosol in unconventional places such as basal poles, possibly attaching to the sparks microtubules (Figure 3E).

Sparks microtubules display SPMTs-like properties

In the absence of γ-tubulin, the formation of SPMTs, ICMTs, spindle microtubules, and centrioles was abolished, and the origin of the abnormally formed long microtubules is unclear. In wild-type parasites, the alveolin network attaches to the growing SPMTs (Mann and Beckers, 2001; Gould *et al.*, 2008; Anderson-White *et al.*, 2011). Interestingly, under U-ExM, budding of the alveolin network denoted by the IMC1 staining was observed on these sparks microtubules suggesting shared properties with the SPMTs (Figure 4A). A hallmark of SPMTs is the appearance of polyglutamylation in a gradient, with the highest intensity at the apical side (Delgado *et al.*, 2024). Similarly, the sparks microtubules emerging from unduplicated centrioles were observed to be gradually polyglutamylated (Figure 4A).

To gain further insight into the molecular identity of these sparks microtubules, we tagged into the γ-tubulin-mAID-HA background four microtubules associated proteins, namely DCX for conoid fibers, ICMAP2 for ICMTs, SPM1 for SPMTs, and EB1 for spindle microtubules (Figure 4B). All four proteins were correctly localized in

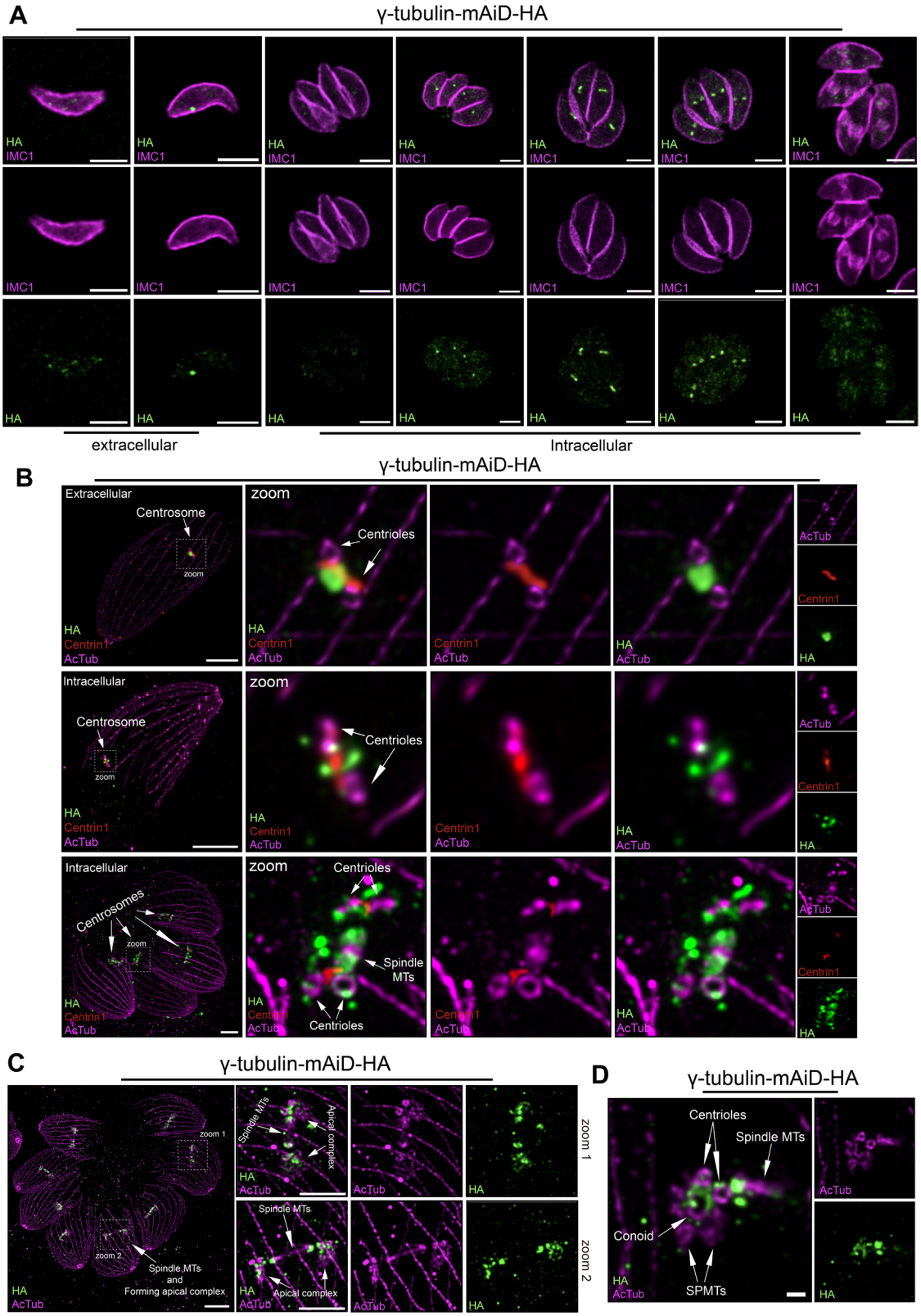

FIGURE 2: Localization of γ-tubulin within *Toxoplasma gondii* cell cycle. (A) Immunofluorescence (IFA) images of γ-tubulin localization in extracellular and intracellular parasites. Scale bar = 3 µm. (B) U-ExM images of the centrosomal organization in regards to centrioles (acetylated tubulin), γ-tubulin and centrin1 protein in extracellular and intracellular parasite. Scale bar = 5 µm. (C) U-ExM images of intracellular dividing parasites showing the γ-tubulin localization during daughter cell cytoskeleton formation. Arrows = Forming conoid. Scale bar = 10 µm. Scale bar zoom regions = 5 µm. (D) U-ExM images showing the localization of γ-tubulin on a forming conoid. Scale bar = 1 µm.

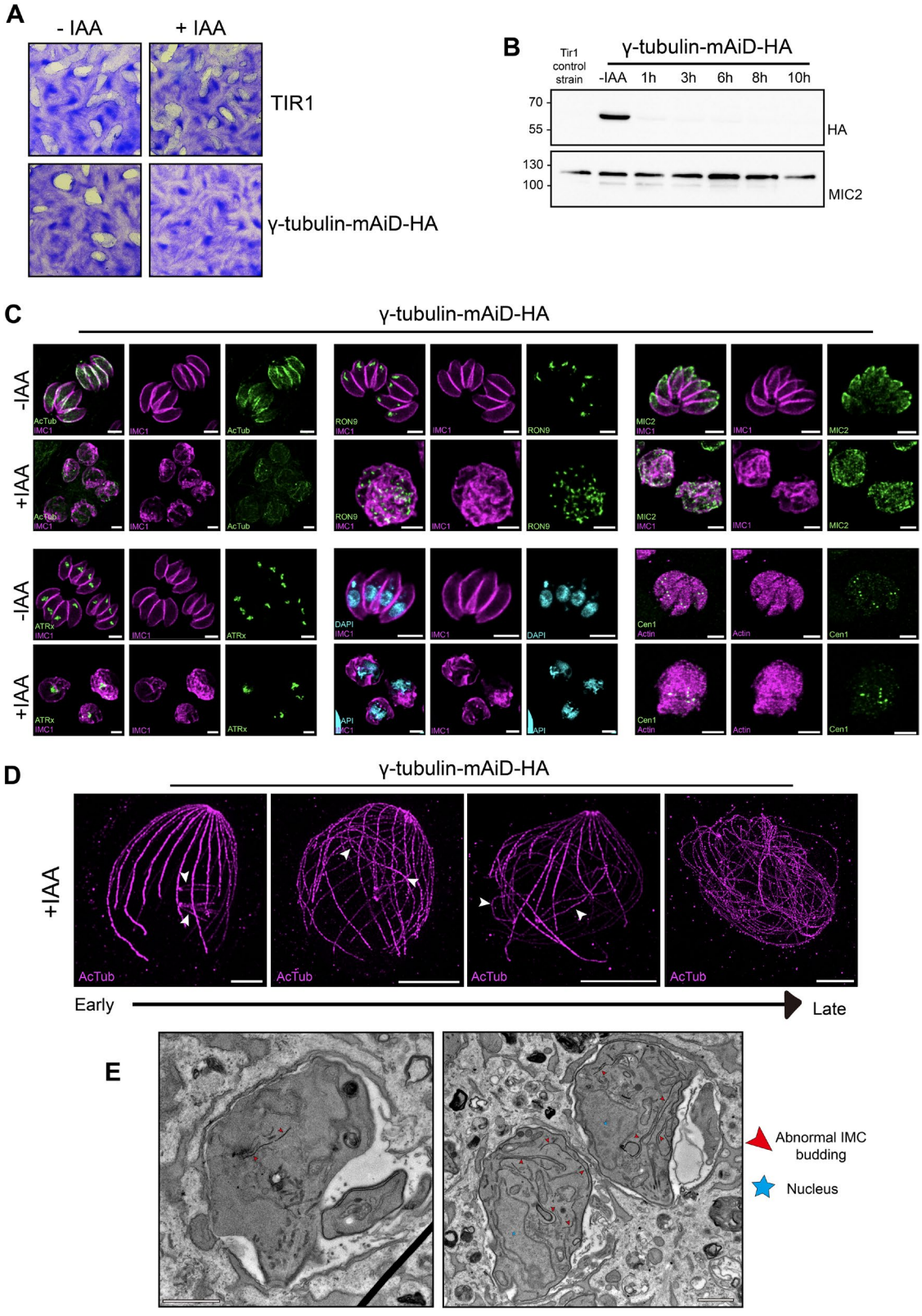

FIGURE 3: γ-tubulin depletion leads to dramatic morphological defects. (A) Images of plaque assay of the γ-tubulin-mAiD-HA and TIR (parental) strain in absence or presence of auxin (IAA). (B) Western-blot analysis of time point protein depletion using anti-HA antibody. MIC2 = loading control. (C) IFA of different cellular structures of *T. gondii* in presence or absence of auxin (IAA). Acetylated Tubulin = AcTub as cytoskeletal marker. Rhoptry Neck protein 9 = RON9 as rhoptry marker. Micronemal protein 2 = MIC2 as microneme marker. Apicoplast-associated thioredoxin family protein = ATRx as apicoplast marker. DAPI as nuclear marker. Centrin1 as centrosomal marker. Scale bar = 3 μm. (D) U-ExM of intracellular dividing parasites depleted of γ-tubulin for 12 h. Scale bar = 10 μm. (E) Electron microscopy images on intracellular dividing parasites. Scale bar = 1 μm

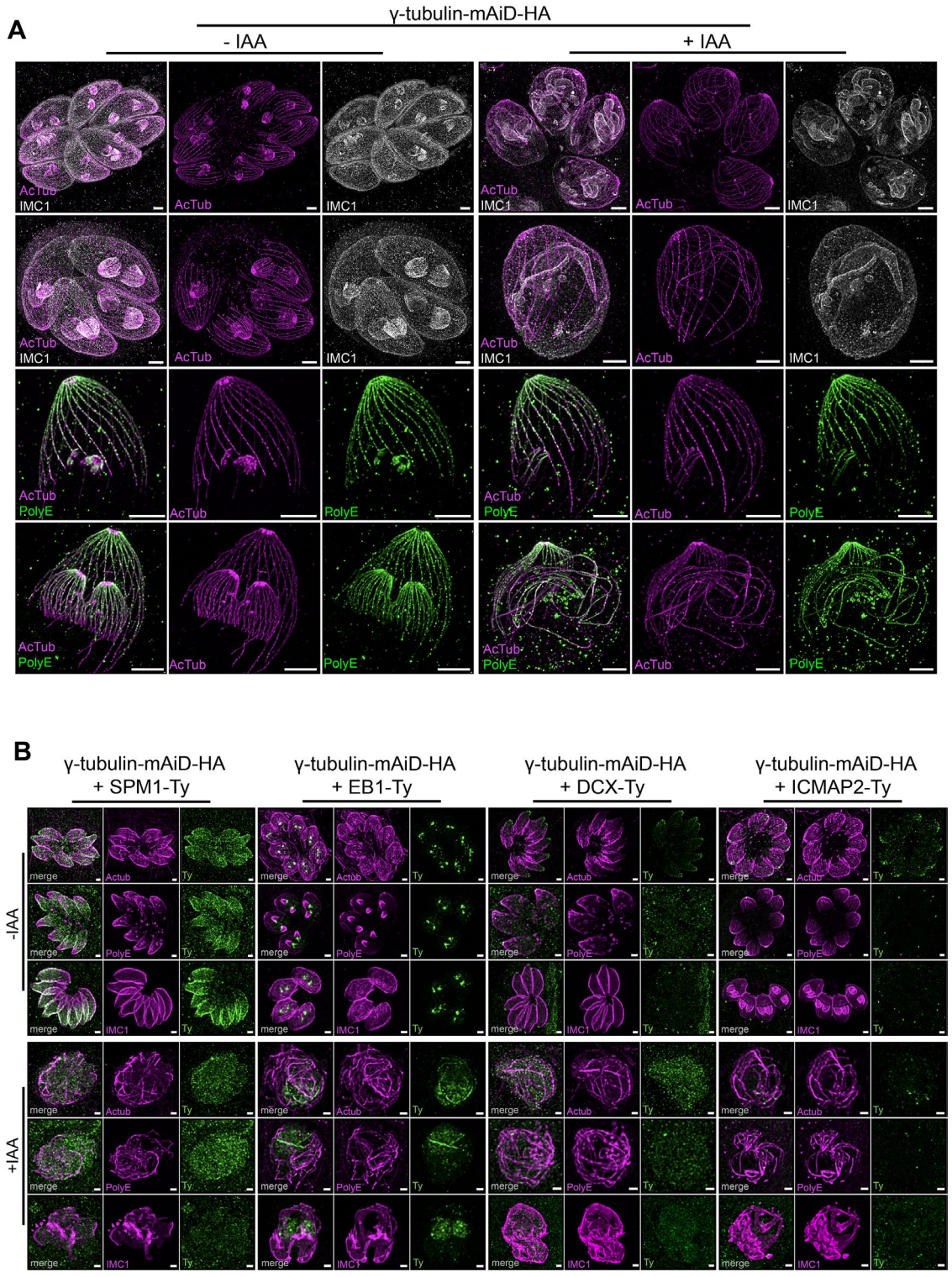

FIGURE 4: Sparks microtubules are divergent microtubules with SPMTs like properties. (A) U-ExM images of intracellular dividing parasites in presence or absence of γ-tubulin. Upper part: IMC1 staining as a marker of alveolin network budding. Lower part: PolyE staining as a marker of specific posttranslational modification of SPMTs. Scale bar = 5 µm. (B) IFA showing the localization of four microtubules associated protein in presence or absence of γ-tubulin in respect to three cellular markers: Acetylated Tubulin, PolyE and IMC1. In +IAA panels, parasites were treated with auxin during 12 h. Scale bar = 1 µm.

their respective compartments, and their correct expression was verified by the western-blot (Figure 4B; Supplemental Figure 2F). In the absence of γ-tubulin, none of the four selected candidates were seen colocalizing with the sparks microtubules defined by the acetylated tubulin and PolyE staining, suggesting that these sparks microtubules are molecularly divergent microtubules (Figure 4B).

The γ-tubulin, in conjunction with GCP proteins, shares localization and phenotypic characteristics

The nucleation of microtubules is a multifactorial process in which γ-tubulin associates with additional proteins called GCPs to provide the molecular scaffold for microtubule nucleation (Moritz *et al.*, 2000; Farache *et al.*, 2016). *T. gondii* possesses genes encoding GCPs albeit a reduced number compared with other organisms, with GCP2, GCP3, and GCP4 being identified (Morlon-Guyot *et al.*, 2017).

To investigate their localization and function, we endogenously tagged the three genes by inserting an mAiD sequence alongside a 3HA-epitope tag in the 3′UTR. We also endogenously Ty-tagged the GCPs in the background of γ-tubulin-mAiD-HA to explore the interactions with γ-tubulin. While we obtained epitope-tagged GCP2 and GCP3, recovery of parasites with tagged GCP4 was unsuccessful (Supplemental Figure 1A).

Parasites depleted of GCP2 or GCP3 for 7 d were unable to form plaque in the fibroblast monolayers, underscoring the essential role of these genes (Figure 5A). Immunofluorescence analysis revealed colocalization of GCP2 and GCP3 with the γ-tubulin signal (Figure 5B). Interestingly, depletion of γ-tubulin led to no detectable signal of GCP2 and GCP3 in immunofluorescence along with reduced protein levels by western blot (Figure 5, C and D). Conditional depletion of GCP2 or GCP3 led to a phenotype resembling that observed for γ-tubulin, characterized by a major morphological defect and adoption of a "bulbous" structure (Supplemental Figure 2G). U-ExM revealed the association of both GCP2 and GCP3 with the forming apical complex during parasite division (Figure 5E). Moreover, similar to γ-tubulin, the signals for GCP2 and GCP3 were consistently observed on the side of the apical complex that was not yet formed, suggesting their role in the very early stages of this structure's formation (Figure 5E).

Cryptosporidium parvum γ-tubulin adopts a dynamic localization throughout the cell cycle

We sought to investigate the conservation of microtubule nucleation in another apicomplexan parasite, *Cryptosporidium parvum*, one of the major causes of children's severe diarrheal disease (Khalil *et al.*, 2018). Despite its reduced genome size, *C. parvum* harbors multiple genes related to microtubule formation suggesting conservation (Figure 6A). This parasite exhibits a polarized morphology that comprises cytoskeletal elements, including the apical complex (conoid, preconoidal rings, and apical polar ring [APR]) and SPMTs (Mageswaran *et al.*, 2021; Wang *et al.*, 2021; Figure 6B).

Commercially available antibodies known to label *T. gondii* tubulin structures were tested on *C. parvum* sporozoites. While antiacetylated tubulin and polyglutamine (polyE) antibodies showed no cross-reactivity, the alpha/beta-tubulin antibodies provided informative staining on *Cryptosporidium* sporozoite. We obtained a similar pattern using the alpha-tubulin or a combination of alpha and beta that resembles the staining with the antibody generated against the *Cryptosporidium* beta-tubulin (Uni *et al.*, 1987; Wang *et al.*, 2021). These antibodies label long and short tubulin filaments with a connection observed between them likely corresponding to SPMTs and the conoid (Figure 6C). U-ExM on extracellular sporozoites revealed additional apical staining as well as staining close to the nucleus (Figure 6C), which is distinct from centrin1 staining, suggesting a unique arrangement of tubulin structures (Figure 6C). iUExM (Louvel *et al.*, 2023) revealed multiple shorter SPMTs in addition to the short and long SPMTs (Figure 6D). These observations mirror previous images of *Cryptosporidium* apical pole acquired by cryo-electron tomography (CryoET; Martinez *et al.*, 2023), where a long SPMT, a short and multiple shorter SPMTs are linked to the APR (blue), followed by the conoid (purple) and the preconoidal rings PCRs (green; Figure 6D; Supplemental Figure 3A).

Despite sharing cytoskeletal morphology with *T. gondii*, *C. parvum* parasites divide by schizogony (English *et al.*, 2022), which involves the formation of eight nuclei before cytokinesis (Figure 6E). To assess the role of γ-tubulin in *C. parvum*, the gene was endogenously epitope-tagged (3HA), allowing its localization within the cell cycle (Supplemental Figure 1B). Interestingly, γ-tubulin protein is undetectable in extracellular sporozoites and in intracellular parasites harboring 1 nucleus contradicting a previous report using an anti-γ-tubulin antibody (Wang *et al.*, 2024; Figure 6F; Supplemental Figure 3B). However, upon nuclear scission, two dots of γ-tubulin were detected on each side of the nuclei, near the centrin1 staining presumably in the centrosomal region (Figure 6F). U-ExM on intracellular dividing parasites revealed γ-tubulin accumulation on both sides of the spindle microtubules preceding their detection (Figure 6G; Supplemental Figure 3C) and without accumulation observed after the budding phase once the cytoskeleton of the merozoites was formed (Figure 6G).

DISCUSSION

Apicomplexan parasites rely on their tubulin cytoskeleton in many aspects of their cell and life cycles. While it has been suggested that γ-tubulin could play the same role in nucleating the spindle microtubules, functional analyses supporting this hypothesis were lacking (Oakley *et al.*, 2015). Additionally, the nucleation of the cortical cytoskeleton, such as the SPMTs, conoid, ICMTs, remained elusive, with some proposing a γ-tubulin-independent process due to its observed localization exclusively to the centrosomal region (Suvorova *et al.*, 2015; Padilla *et al.*, 2024). We present evidence for the conserved localization of the γ-tubulin in two apicomplexan parasites *T. gondii* and *C. parvum,* in the formation of spindle microtubules during nucleus scission. Applying U-ExM allowed to explore the early formation of the apical complex and cortical cytoskeleton, revealing the transient localization of γ-tubulin to these structures, presumably to control their nucleation process. The association of γ-tubulin with the forming apical complex appears to be very transient, always on the opposite side as the tubulin staining suggesting a role in the initiation but not for elongation of microtubules. Importantly, we found that the reduced set of γ-tubulin complex proteins (GCPs) originally identified in an in silico analysis recapitulated the same localization and phenotype as γ-tubulin, emphasizing their functional conservation (Morlon-Guyot *et al.*, 2017).

Depletion of γ-tubulin in parasites resulted in dramatic morphological impairments, primarily due to the lack of nuclear scission and cortical/conoid cytoskeleton formation. However, residual microtubules could still be observed in these defective parasites. In the absence of γ-tubulin, microtubules emerge from unduplicated centrioles, and as the cell-cycle progresses, these microtubules end elongate to an extreme length, forming abnormal structures that twirled around the misshaped parasite. These microtubules are associated alveolin network budding and exhibit gradual polyglutamylation. However, none of the four microtubule-associated proteins tagged in the γ-tubulin-mAID-HA background localized on these microtubules, suggesting a divergent composition with SPMTs-like properties. The origin and nucleation process of these abnormal microtubules, which appeared to be γ-tubulin-independent, remain open questions, warranting further investigation.

In our investigation of *C. parvum*, we aimed to enhance our understanding of its cytoskeleton organization. Recent advances in Cryo-ET have filled considerably the gap of knowledge on the cytoskeleton of *C. parvum* (Mageswaran *et al.*, 2021; Wang *et al.*, 2021;

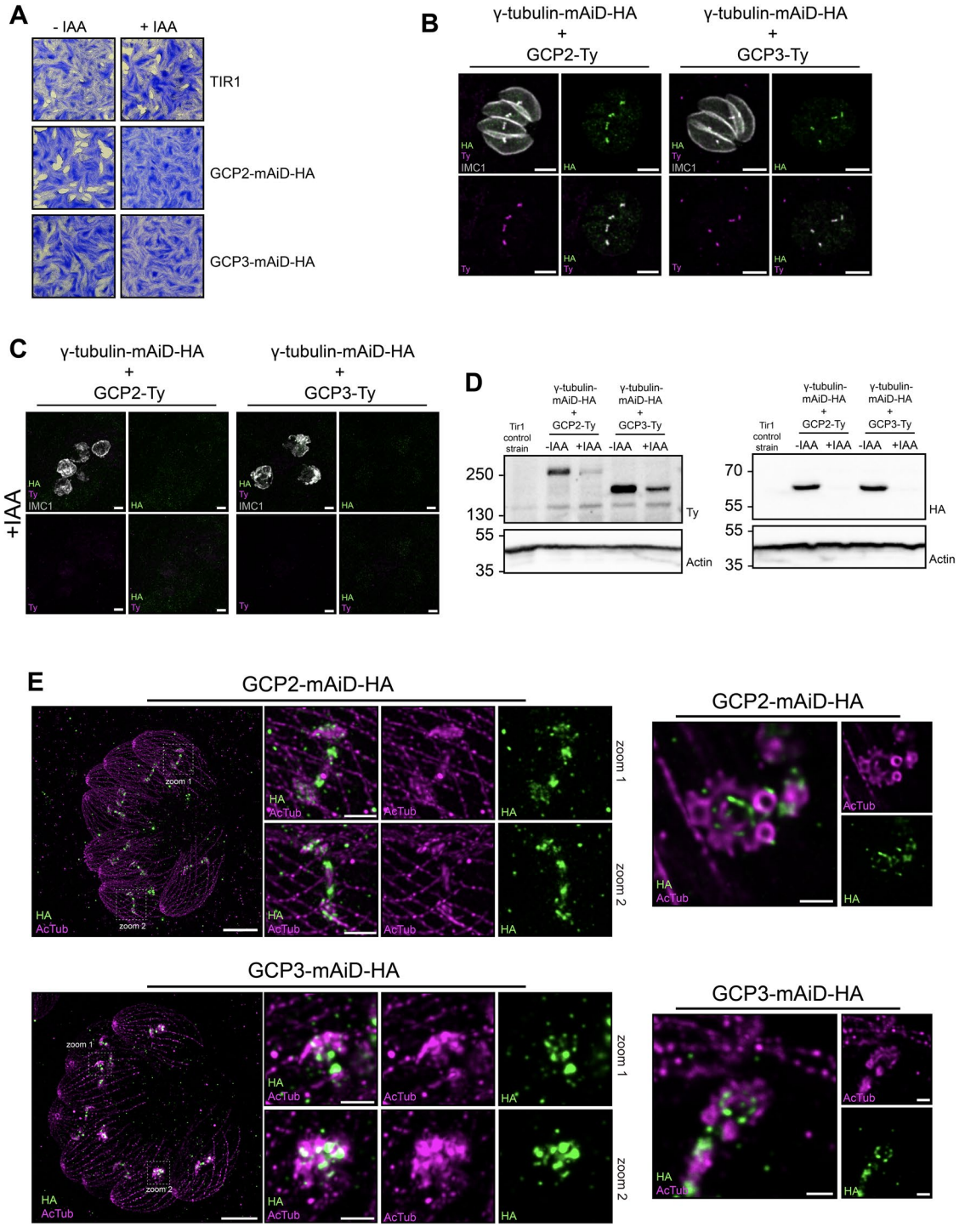

FIGURE 5: Nucleation of microtubules involve a concerted action of γ-tubulin and GCP proteins. (A) Images of plaque assay of the GCP2-mAiD-HA, GCP3-mAiD-HA and TIR (parental) strain in absence or presence of auxin (IAA). (B) IFA images of the colocalization of γ-tubulin with GCP2 or GCP3 protein in intracellular dividing parasite. Scale bar = 3 μm. (C) IFA images of the intracellular dividing parasites depleted for γ-tubulin showing the loss of GCPs signal. (D) Western-blot analysis of protein depletion using Ty-antibody (left panel) and anti-HA antibody (right panel). Actin = loading control. IAA treatment for 12 h. (E) Expansion microscopy images of intracellular dividing parasites showing the localization of GCP2 and GCP3 during the formation of the daughter cytoskeleton (left panel) and on the forming conoid (right panel) Scale bar = 10 μm. Scale bar zoom regions = 2 μm

Martinez *et al.*, 2023), although some aspects remain contentious in the literature. Indeed, *Cryptosporidium* sporozoite was first suggested to possess numerous long SPMTs by EM analyses (Uni *et al.*, 1987; Baba *et al.*, 2008). However, the IMC surface filaments were likely misinterpreted as SPMTs (Martinez *et al.*, 2023). Additionally, some studies reported the presence of two central microtubules, which are not consistently identified as SPMTs (Uni *et al.*, 1987; Wang *et al.*, 2021). To clarify these discrepancies and provide a

detailed view of the tubulin cytoskeleton in *Cryptosporidium* sporozoites, we employed U-ExM and iU-ExM. We observe two long SPMTs one longer than the other and attached to the APR. We also observe the architecture of the sporozoites centrosome with a conserved localization of the centrin1 as well as numerous short SPMTs below the APR and the extruded conoid consistent with previous EM and Cryo-ET analysis (Uni *et al*., 1987; Martinez *et al*., 2023).

Given that nucleation of the tubulin cytoskeleton of *C. parvum* remains an open question, we investigated the role of γ-tubulin. Contrary to previous observations using a commercial anti-γ-tubulin antibody, endogenous tagging of the gene shows no accumulation of γ-tubulin at the apical pole of sporozoites (Wang *et al*., 2024). This observation aligns with the absence of microtubule nucleation at this stage. Mass spectrometry analysis further supported the absence of γ-tubulin complex proteins in sporozoites, suggesting no active nucleation in these parasites (Guérin *et al*., 2023). Additionally, γ-tubulin was observed to accumulate in intracellular parasites during merogony before the formation of the spindle microtubules, presumably to nucleate them for nuclear division. As soon as the eight nuclei were separated the γ-tubulin signal disappeared. However, in contrast to *T. gondii,* we were not able to detect γ-tubulin in the forming cytoskeleton of merozoites. This discrepancy could be attributed to the challenge of catching merozoites' cytoskeleton formation or that their nucleation is guided by a γ-tubulin independent mechanism.

Recent advances, such as the implementation of a conditional knockdown system combined with advanced microscopy techniques, should help to unravel the formation of *C. parvum* tubulin cytoskeleton (Choudhary Hadi *et al*., 2020; Tandel *et al*., 2023; Xu *et al*., 2024).

MATERIALS AND METHODS

T. gondii maintenance in tissue culture

Toxoplasma gondii tachyzoites were amplified in HFFs (ATCC) in Dulbecco's Modified Eagle's Medium (DMEM; Life Technologies) supplemented with 5% of fetal calf serum (FCS; Life Technologies), 2 mM glutamine and 25 µg/ml gentamicin (Life Technologies). Parasites and HFFs were maintained at 37°C with 5% CO_2.

C. parvum strain lineage, host cell culture, and mouse model

C. parvum oocysts (Iowa II strain) used to make the transgenic line were purchased from the Bunchgrass Farms Deary, ID.

Cell lines used for this study were HCT8 (ATCC: CCL-244) purchased from ATCC. The cells were cultured in DMEM supplemented with 10% bovine serum.

Ifng –/– mice with C57BL/6J background were bought from Charles River Laboratories and were bred at the University of Geneva. Four male mice at the age of 6 wk were used to infect with the *C. parvum* transgenic line. Feces were collected from d 5 to d 21. All the animal studies performed at the University of Geneva are complied with the Swiss National Institutional Guidelines on Animal Experimentation and were approved by the respective Swiss Cantonal Veterinary Office Committees for Animal Experimentation (GE276A).

Generation of transgenic *T. gondii* lines

Freshly egressed tachyzoites were transfected by electroporation (Soldati and Boothroyd, 1993).

All the strains used in this study were constructed using CRISPR-mediated homology directed repair. For construction of 3'-insertional epitope tagging, 40 µg pU6-Universal (pU6-Universal was a gift from Sebastian Lourido, Addgene plasmid # 52694) bearing the gRNA to target the 3'UTR of gene of interest (GOI) was transfected together with PCR product containing homology regions for the selected gene. To generate the knockout lines, a plasmid bearing dual gRNA targeting at 5'- and 3'-locus of GOI was cotransfected with PCR product encoding DHFR resistance cassette. For enrichment of transfected population, parasites carrying an HXGPRT cassette were selected with 25 mg/ml of mycophenolic acid (MPA) and 50 mg/ml xanthine. Parasites carrying a DHFR cassette were selected with 1 µg/ml of pyrimethamine. All the assays involving AID-based conditional knockdown system, the protein depletion was achieved by adding 500µM of auxin (IAA; Brown *et al*., 2018)

Generation of transgenic *C. parvum* transformants

Twenty million *C. parvum* oocysts were excysted and electroporated as previously described (Guérin *et al*., 2021). Briefly, a guide RNA corresponding to the 3'UTR of cgd7_1980 (AGAAAGGAGAAGTACGCGGA) was inserted by ligation in the Cas9 vector. Fifty milligrams of the corresponding vector was precipitated with 200 ul of repair template PCR containing 30 bp homology with cgd7_1980, the triple hemagglutinin tag, a generic 3' UTR and the nanoluciferase-neomycin cassette under the enolase promoter (Supplemental Table1). Transfected parasites were gavaged into ifng –/– mice and paromomycin in the mice drinking water was used to select resistant transformants. Shedded oocysts from the feces were collected and purified using sucrose floatation and cesium chloride gradient. They were stored in PBS at 4°C until further use.

Genomic PCR analysis to confirm correct integration in the genome

For both *T. gondii* and *C. parvum* genomic DNA of the parasites was extracted using Wizard SV genomic DNA purification system ki (*T. gondii*) or Quick-DNA Fecal/Soil Microbe Microprep kit (*C. parvum*). For *T. gondii* PCR primers were designed to bind outside the 30 bp homology arms in 5' region as well as to the mAiD cassette or DHFR resistance cassette. For *C. parvum*, PCR primers were designed to bind outside the 30 bp homology arms in 5' and 3' region as well as to the triple HA tag and the Neomycin resistance cassette inserted. For both parasites an independent strain was used as a PCR control (Supplemental Figure 1).

Indirect immunofluorescence Assay (*T. gondii*)

Parasites were fixed using a mix 4% paraformaldehyde; 0,05% Glutaraldehyde during 10 min at room temperature. Following fixation, they were permeabilized by 20-min incubation with PBS-Tx100 0,2% at room temperature. Parasites were blocked during 20 min by PBS-BSA (bovine serum albumin) 5% followed by incubation with the primary antibodies during 1 h in PBS-BSA 2%. Coverslips were washed three times during 5 min by PBS-Tx100 0,2% and then incubated with secondary antibodies diluted in PBS-BSA 2% during 1 h at room temperature. Coverslips were washed three times during 5 min by PBS-Tx100 0,2% and then mounted using Fluoromount G on microscope slides.

Indirect immunofluorescence Assay (*C. parvum*)

Oocysts were bleached using 2.7% bleach and were excysted with 0.8% sodium taurocholate for 10 min. To image sporozoites, excysted oocysts were incubated for 1 h at 37°C in PBS. Following incubation, they were allowed to settle onto poly-L-lysine coated coverslips for 30 min. To investigate intracellular parasites, they were allowed to infect human adeno carcinoma HCT-8 cells for various times mentioned in individual experiments. These were then fixed with 4% paraformaldehyde for 15 min or with methanol for 7 min at

A

Name	ID ToxoDB	ID CryptoDB	Evalue
Alpha tubulin	316400	cgd4_2860	0
Beta tubulin	266960	cgd6_4760	0
Gamma tubulin	226870	cgd7_1980	0
GCP2	263510	cgd7_3060	2e-05
GCP3	310130	cgd6_3410	8e-10
Centrin1	247230	cgd3_1270	1e-74

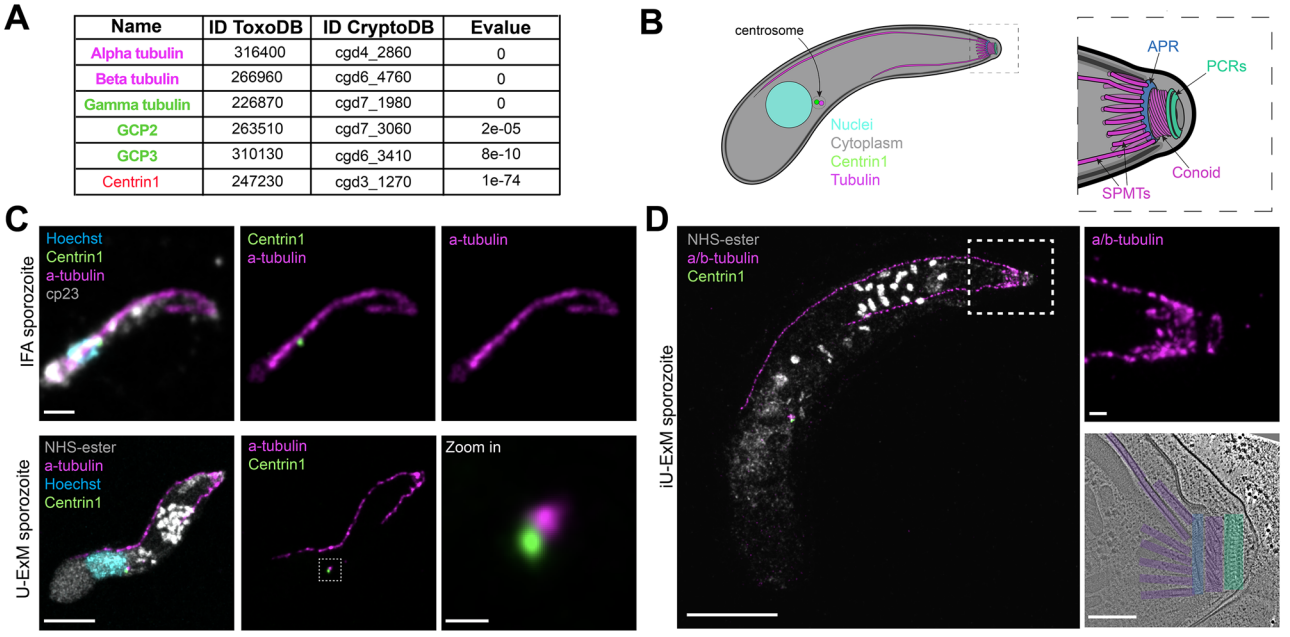

E

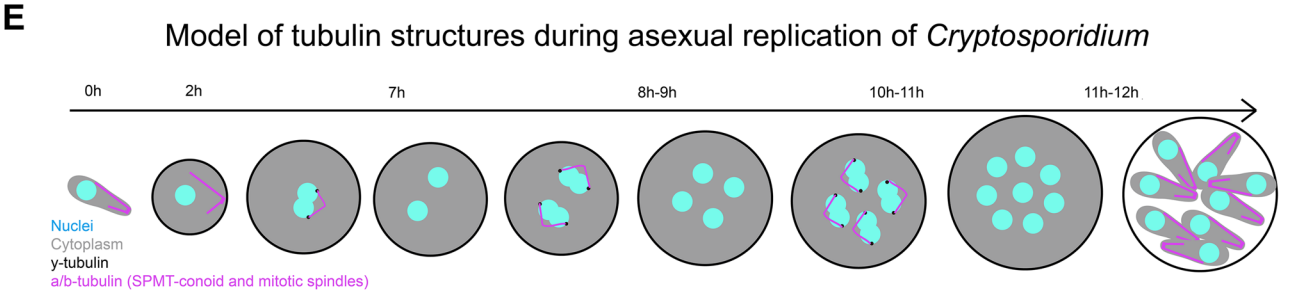

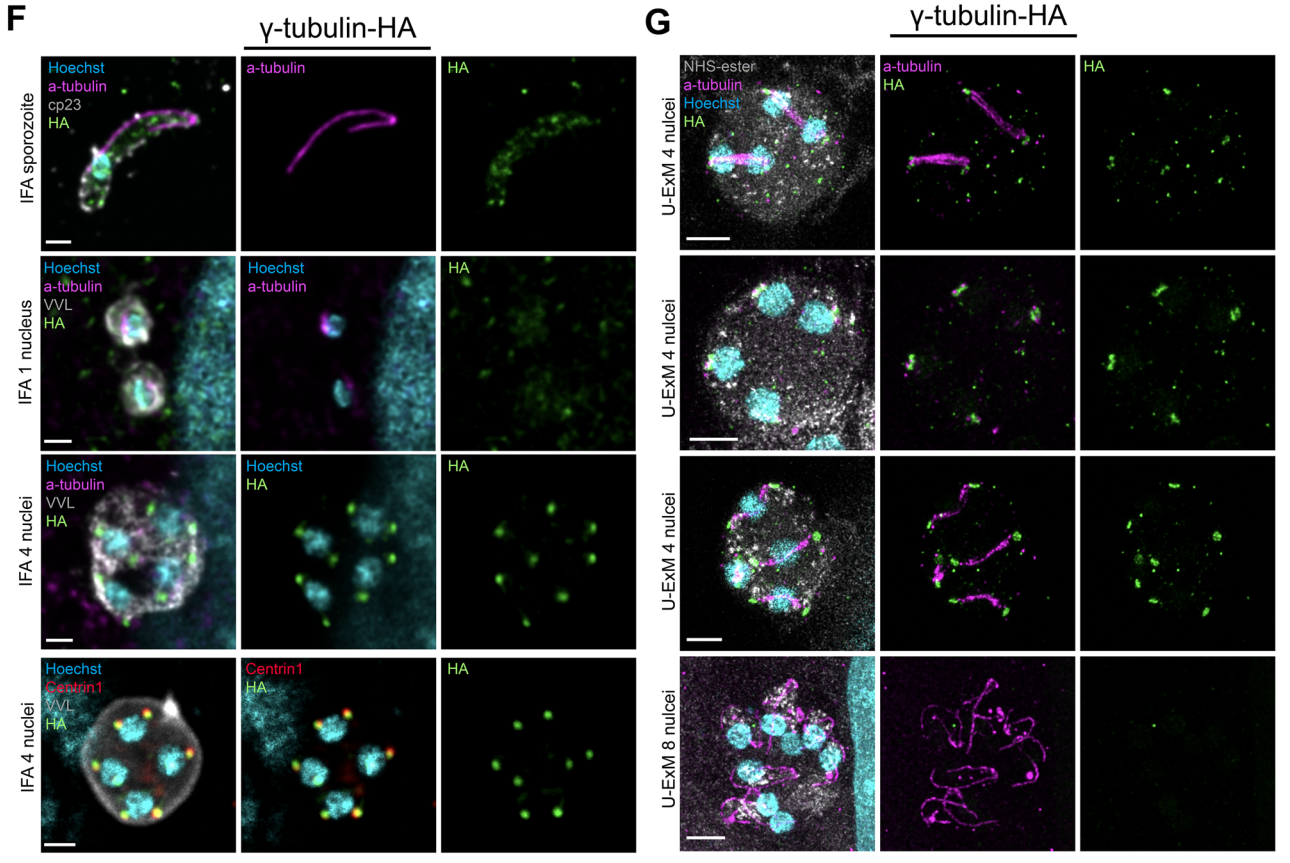

–20°C and permeabilized with 0.5% Triton X-100 for 15 min. Samples were blocked with 4% BSA for 1 h at room temperature, following by 1 h of primary antibodies diluted in 1% BSA. After being washed three times with PBS, secondary antibodies were diluted in 1% BSA for 1 h at room temperature (Dilution of antibodies and dyes used in supplemental table). The cells were stained with the DNA dye Hoechst for 5 min which was diluted in PBS. A three times wash with PBS is followed and the coverslips were mounted on glass slides with Fluoromount. The cells were imaged using the Leica TCS SP8 microscopy with the lens HC PL Apo 100x/1.40 Oil CS2.

Expansion microcopy (*T. gondii*)

The expansion microscopy protocol applied to *Toxoplasma gondii* tachyzoites was followed as described in this study (Dos Santos Pacheco and Soldati-Favre, 2021). Coverslips containing intracellular dividing parasites were incubated in PBS containing 0.7% formaldehyde and 1% acrylamide for 3 h at 37°C. Polymerization of expansion gel were performed on ice containing monomer solution (19% sodium acrylate/10% acrylamide/0.1% (1,2-Dihydroxyethylene) bisacrylamide), 0.5% ammonium persulfate (APS) and 0.5% tetramethyl ethylenediamine (TEMED) as described in this study (Louvel *et al.*, 2023). Fully polymerized gels were denaturated at 85°C for 90 min in the denaturation buffer (200 mM SDS, 200 mM NaCl, 50 mM Tris, pH = 6.8) and expanded in pure H_2O overnight.

On the next day, the expansion ratio of fully expanded gels was determined by measuring the diameter of gels. Well expanded gels were shrunk in PBS and stained with primary and secondary antibodies diluted in freshly prepared PBS/BSA 2% at 37°C for 2 h. Three washes with PBS/0.1% Tween for 10 min were performed after primary and secondary antibody staining. Stained gels were expanded again in pure H_2O overnight for further imaging. All U-ExM images used in this study were acquired using Leica TCS SP8 microscopy with the lens HC PL Apo 100x/1.40 Oil CS2. Images were taken with Z-stack and deconvolved with the built-in setting of Leica LAS X or with Huygens software. Final images were processed with ImageJ and the maximum projected images were presented in this study.

Expansion microcopy (*C. parvum*)

U-ExM was applied as described for *Toxoplasma*. Parasites were excysted and fixed the same way as mentioned for IFA. Samples were embedded overnight in a mixture of acrylamide and formaldehyde which adds a molecular anchor to each protein and thus, crosslinking of protein groups was avoided. The formed gel was transferred into denaturation buffer and denatured at 95°C. Following denaturation, the gels were then placed in water to expand around four times its size. The gels were shrunk with PBS before incubation for 3 h with primary antibodies, three washes with PBS-Tween 0.5% and incubation for 3 h with secondary antibodies containing Hoechst DNA dye. The gels were bathed in water for expansion. All U-ExM images used in this study were acquired using Leica TCS SP8 microscopy with the lens HC PL Apo 100x/1.40 Oil CS2. Images were taken with Z-stack and deconvolved with the build-in setting of Leica LAS X or with Huygens software. Final images were processed with ImageJ and the maximum projected images were presented in this study.

Iterative Ultrastructure Expansion Microscopy (iU-ExM)

Iterative ultrastructure expansion microscopy was applied as described (Louvel *et al.*, 2023). Parasites were excysted, fixed, and anchored the same way as mentioned for U-ExM. The first monomer solution was added to fill in the space of the gelation chamber. Following an incubation of 15 min on ice, an incubation at 37°C for 45 min was completed. The formed gels were transferred into the denaturation buffer and incubated at 85°C for 90 min. The gels were placed in water to expand five to six times their size and were shrunk with PBS to apply primary and secondary antibodies. The gels were bathed in water again and were cut into pieces that were incubated three times for 10 min on an agitating platform with activated neutral gel. The gels were dried by sliding it onto the microscope slide. A coverslip was placed on top and the chamber was incubated at 37°C for 1 h. The gel was bathed in the combination of acrylamide and formaldehyde for overnight at 37°C under agitation. The following day, the gel was washed twice with 1x PBS for 30 min before applying the 3rd monomer solution to achieve an expansion factor of approximately 16x. The gel was washed three times for 10 min under agitation on ice and was dried on the microscope slide. A coverslip was placed on top within a chamber and incubated for 1 h at 37°C. The gel was bathed in 200 mM NaOH solution for 1 h under agitation at RT and was washed in 1x PBS for 20 min until the pH reaches 7. The last round of expansion was carried out with water and cells were imaged using Leica TCS SP8 microscopy with the lens HC PL Apo 100x/1.40 Oil CS2. Images were taken with Z-stack and deconvolved with the built-in setting of Leica LAS X or with Huygens software. Final images were processed with ImageJ and the maximum projected images were presented in this study.

Plaque assay

HFF monolayers were infected with a serial dilution of *T. gondii* tachyzoites and grown for 7 d at 37°C. Cells were fixed with using paraformaldehyde-glutaraldehyde for 10 min followed by a neutralization by PBS/Glycine 0.1M. The fixed monolayer was then stained with crystal violet for 2 h and then washed three times with PBS.

Western blot analysis for monitoring auxin-induced protein degradation

HFF monolayers seeded in 6-cm petri dishes were infected with freshly egressed parasites and grown for a defined time (1 h to 10 h) in absence or presence of IAA (500 μM). Cells containing the parasites were scrapped and pelleted at 1200 rpm and resuspend in protein loading buffer containing 2% SDS and boiled for 15 min at

FIGURE 6: Analysis of *Cryptosporidium parvum* cytoskeleton and γ-tubulin dynamic during merogony. (A) Table of conservation of proteins involved in cytoskeleton formation in *T. gondii* and *C. parvum*. (B) Schematic representation of *C. parvum* sporozoite cytoskeletal architecture. Right panel = zoom in the apical region. (C) Upper panel = IFA image of *C. parvum* sporozoite. Scale bar = 1 μm. Lower panel = U-ExM image of *C. parvum* sporozoite. Scale bar = 5 μm. Zoom in scale bar = 0.5 μm. (D) Iterative U-ExM image of *C. parvum* sporozoite. Scale bar = 15 μm. Zoom in scale bar = 1 μm. Lower right panel = Cryoelectron microscopy tomogram slice of the apical end of *C. parvum* sporozoite. Scale bar = 0.2 μm. (E) Schematic representation of *C. parvum* asexual replication at different time points. (F) IFA images showing the γ-tubulin-HA localization in extracellular and intracellular parasites. Scale bar = 1μm. VVL: Vicia villosa lectin used as a PV marker. (G) U-ExM images of the γ-tubulin-HA localization in intracellular parasites at different points of the asexual replication. Scale bar = 5 μm.

95°C. Protein depletion was assessed by Western-Blot using anti-HA antibody against the protein of interest and anti-MIC2 as a loading control.

ACKNOWLEDGMENTS

We thank for their technical assistance and imaging analysis, the team at the Bioimaging Core Facility, François Prodon, Olivier Brun, and Nicolas Liaudet.

We generously thank Yi-Wei Chang for allowing us to use a tomogram image of *Cryptosporidium parvum*. The project is funded by the Swiss National Science Foundation to D.S.F. (310030_215445) and to A.G. (PR00P3_208568).

REFERENCES

Aher A, Urnavicius L, Xue A, Neselu K, Kapoor TM (2023). Structure of the γ-tubulin ring complex-capped microtubule. bioRxiv, https://doi.org/10.1101/2023.11.20.567916.

Anderson-White BR, Douglas Ivey F, Cheng K, Szatanek T, Lorestani A, Beckers CJ, Ferguson DJP, Sahoo N, Gubbels M-J (2011). A family of intermediate filament-like proteins is sequentially assembled into the cytoskeleton of *Toxoplasma gondii*. Cellular Microbiol, 13, 18–31.

Baba E, Kimata I, Matsubayashi M, Nakagawa H, Sasai K, Takase H, Tani H (2008). Electron microscopic observation of cytoskeletal frame structures and detection of tubulin on the apical region of *Cryptosporidium parvum* sporozoites. Parasitology, 135, 295–301.

Ben Chaabene R, Lentini G, Soldati-Favre D (2020). Biogenesis and discharge of the rhoptries: Key organelles for entry and hijack of host cells by the Apicomplexa. Mol Microbiol 115, 453–465.

Brown KM, Long S, Sibley LD (2018). Conditional knockdown of proteins using Auxin-inducible Degron (AID) fusions in *Toxoplasma gondii*. Bio Protoc 8, e2728.

Choudhary Hadi H, Maria GN, Gartlan Brina E, Rose S, Vinayak S (2020). A conditional protein degradation system to study essential gene function in *Cryptosporidium parvum*. mBio, 11, e01231-20.

Delgado ILS, Gonçalves J, Fernandes R, Zúquete S, Basto AP, Leitão A, Soares H, Nolasco S (2024). Balancing act: Tubulin glutamylation and microtubule dynamics in *Toxoplasma gondii*. Microorganisms, 12, 488.

Dos Santos Pacheco N, Brusini L, Haase R, Tosetti N, Maco B, Brochet M, Vadas O, Soldati-Favre D (2022). Conoid extrusion regulates glideosome assembly to control motility and invasion in Apicomplexa. Nat Microbiol, 7, 1777–1790.

Dos Santos Pacheco N, Soldati-Favre D (2021). Coupling auxin-inducible degron system with ultrastructure expansion microscopy to accelerate the discovery of gene function in *Toxoplasma gondii*. In: Parasite Genomics: Methods and Protocols, ed. LM de Pablos and J Sotillo, New York, NY: Springer, 121–137.

Dos Santos Pacheco N, Tell i Puig P, Guérin A, Martinez M, Maco B, Tosetti N, Delgado-Betancourt E, Lunghi M, Striepen B, Chang Y-W, Soldati-Favre D (2024). Sustained rhoptry docking and discharge requires Toxoplasma gondii intraconoidal microtubule-associated proteins. Nat Commun 15, 379.

Dos Santos Pacheco N, Tosetti N, Koreny L, Waller R. F, Soldati-Favre D (2020). Evolution, composition, assembly, and function of the Conoid in Apicomplexa. Trends Parasitol, 36, 688–704.

Dubois DJ, Soldati-Favre D (2019). Biogenesis and secretion of micronemes in *Toxoplasma gondii*. Cell Microbiol, 21, e13018.

English ED, Guérin A, Tandel J, Striepen B (2022). Live imaging of the *Cryptosporidium parvum* life cycle reveals direct development of male and female gametes from type I meronts. PLOS Biology, 20, e3001604.

Farache D, Jauneau A, Chemin C, Chartrain M, Rémy MH, Merdes A, Haren L (2016). Functional analysis of γ-tubulin complex proteins indicates specific lateral association via their n-terminal domains. J Biol Chem, 291, 23112–23125.

Gould SB, Tham W-H, Cowman AF, McFadden GI, Waller RF (2008). Alveolins, a new family of cortical proteins that define the protist infrakingdom Alveolata. Mol Biol Evol, 25, 1219–1230.

Green JL, Wall RJ, Vahokoski J, Yusuf NA, Ridzuan MAM, Stanway RR, Stock J, Knuepfer E, Brady D, Martin SR, *et al.* (2017). Compositional and expression analyses of the glideosome during the Plasmodium life cycle reveal an additional myosin light chain required for maximum motility. J Biol Chem, 292, 17857–17875.

Gubbels MJ, Keroack CD, Dangoudoubiyam S, Worliczek HL, Paul AS, Bauwens C, Elsworth B, Engelberg K, Howe DK, Coppens I, Duraisingh MT (2020). Fussing about fission: Defining variety among mainstream and exotic apicomplexan cell division modes. Front Cell Infect Microbiol, 10, 269.

Guérin A, Roy NH, Kugler EM, Berry L, Burkhardt JK, Shin J-B, Striepen B (2021). Cryptosporidium rhoptry effector protein ROP1 injected during invasion targets the host cytoskeletal modulator LMO7. Cell Host & Microbe, 29, 1407–1420.e5.

Guérin A, Strelau KM, Barylyuk K, Wallbank BA, Berry L, Crook OM, Lilley KS, Waller RF, Striepen B (2023). Cryptosporidium uses multiple distinct secretory organelles to interact with and modify its host cell. Cell Host & Microbe, 31, 650–664.e6.

Khalil IA, Troeger C, Rao PC, Blacker BF, Brown A, Brewer TG, Colombara DV, Hostos ELD, Engmann C, Guerrant RL, *et al.* (2018). Morbidity, mortality, and long-term consequences associated with diarrhoea from Cryptosporidium infection in children younger than 5 years: a meta-analyses study. Lancet Glob Health, 6, e758–e768.

Louvel V, Haase R, Mercey O, Laporte MH, Eloy T, Baudrier É, Fortun D, Soldati-Favre D, Hamel V, Guichard P (2023). iU-ExM: nanoscopy of organelles and tissues with iterative ultrastructure expansion microscopy. Nat Commun, 14, 7893.

Mageswaran SK, Guerin A, Theveny LM, Chen WD, Martinez M, Lebrun M, Striepen B, Chang YW (2021). In situ ultrastructures of two evolutionarily distant apicomplexan rhoptry secretion systems. Nat Commun, 12, 4983.

Mann T, Beckers C (2001). Characterization of the subpellicular network, a filamentous membrane skeletal component in the parasite *Toxoplasma gondii*. Mol Biochem Parasitol, 115, 257–268.

Martinez M, Mageswaran SK, Guérin A, Chen WD, Thompson CP, Chavin S, Soldati-Favre D, Striepen B, Chang YW (2023). Origin and arrangement of actin filaments for gliding motility in apicomplexan parasites revealed by cryo-electron tomography. Nat Commun, 14, 4800.

Moritz M, Braunfeld MB, Guénebaut V, Heuser J, Agard DA (2000). Structure of the γ-tubulin ring complex: a template for microtubule nucleation. Nat Cell Biology, 2, 365–370.

Morlon-Guyot J, Francia ME, Dubremetz J-F, Daher W (2017). Towards a molecular architecture of the centrosome in *Toxoplasma gondii*. Cytoskeleton, 74, 55–71.

Oakley BR, Paolillo V, Zheng Y (2015). γ-Tubulin complexes in microtubule nucleation and beyond. Mol Biol Cell, 26, 2957–2962.

Opitz C, Soldati D (2002). The glideosome, a dynamic complex powering gliding motion and host cell invasion by *Toxoplasma gondii*. Science 45, 597–604.

Padilla LFA, Murray JM, Hu K (2024). The initiation and early development of the tubulin-containing cytoskeleton in the human parasite *Toxoplasma gondii*. Mol Biol Cell 35, ar37.

Soldati D, Boothroyd JC (1993). Transient transfection and expression in the obligate intracellular parasite *Toxoplasma gondii*. Science, 260, 349–352.

Suvorova ES, Francia M, Striepen B, White MW (2015). A novel bipartite centrosome coordinates the apicomplexan cell cycle. PLoS Biology, 13, e1002093.

Tandel J, Walzer Katelyn A, Byerly Jessica H, Pinkston B, Beiting Daniel P, Striepen B (2023). Genetic ablation of a female-specific Apetala 2 transcription factor blocks oocyst shedding in *Cryptosporidium parvum*. mBio, 14, e03261–e03322.

Tell i Puig P, Soldati-Favre D (2024). Roles of the tubulin-based cytoskeleton in the *Toxoplasma gondii* apical complex. Trends Parasitol 40, 401–415.

Thawani A, Petry S (2021). Molecular insight into how γ-TuRC makes microtubules. J Cell Sci, 134, jcs245464.

Uni S, Iseki M, Maekawa T, Moriya K, Takada S (1987). Ultrastructure of Cryptosporidium muris (strain RN 66) parasitizing the murine stomach. Parasitol Res, 74, 123–132.

Wang C, Wang D, Nie J, Gao X, Yin J, Zhu G (2021). Unique tubulin-based structures in the zoonotic apicomplexan parasite *Cryptosporidium parvum*. Microorganisms 9, 1921.

Wang D, Jiang P, Wu X, Zhang Y, Wang C, Li M, Liu M, Yin J, Zhu G (2024). Requirement of microtubules for secretion of a micronemal protein CpTSP4 in the invasive stage of the apicomplexan *Cryptosporidium parvum*. mBio, 15, e03158–e03223.

Xu R, Beatty WL, Greigert V, Witola WH, David Sibley L (2024). Multiple pathways for glucose phosphate transport and utilization support growth of Cryptosporidium parvum. Nat Commun, 15, 380.

Zheng Y, Wong ML, Alberts B, Mitchison T (1995). Nucleation of microtubule assembly by a γ-tubulin-containing ring complex. Nature, 378, 578–583.